Article

Annual Comparison of the Atmospheric Urban Heat Island in Rome (Italy): An Assessment in Space and Time

Edoardo De Cristo [1], Luca Evangelisti [2,*], Gabriele Battista [2], Claudia Guattari [3], Roberto De Lieto Vollaro [2] and Francesco Asdrubali [4]

1   Department of Engineering, Niccolò Cusano University, Via Don Carlo Gnocchi 3, 00166 Rome, Italy; edoardo.decristo@unicusano.it

2   Department of Industrial, Electronic and Mechanical Engineering, Roma TRE University, Via Vito Volterra 62, 00146 Rome, Italy; gabriele.battista@uniroma3.it (G.B.); roberto.delietovollaro@uniroma3.it (R.D.L.V.)

3   Department of Philosophy, Communication and Performing Arts, Roma TRE University, Via Ostiense 139/10, 00154 Rome, Italy; claudia.guattari@uniroma3.it

4   Department of International Human and Social Sciences, Perugia Foreigners' University, Piazza Fortebraccio 4, 06122 Perugia, Italy; francesco.asdrubali@unistrapg.it

*   Correspondence: luca.evangelisti@uniroma3.it

Abstract: This study examined the atmospheric urban heat island (UHI) phenomenon within the city of Rome (Italy) and its effects on building energy demand. Weather data from 2020 and 2022 collected from six meteorological stations were considered. A Geographic Information System (GIS) was used to analyze the landscape, correlating the percentage of impermeable surfaces with UHI intensity values in each area. Dynamic simulations were conducted using different climatic data to estimate the heating and cooling energy demands for two representative residential buildings. The findings revealed significant differences in the climatic conditions between urban and rural areas, primarily due to temperature increases. The UHI intensities reached maximum values of 4.67 °C and 3.54 °C in 2020 and 2022. In urban areas, the UHI has positive effects on the heating energy demand but results in a significant increase in energy demand for cooling. Considering a building type constructed between 1900 and 1950, a variation of up to 33.03% in the heating energy demand in urban areas compared to rural areas was calculated, along with a variation of up to 81% for cooling. In contrast, considering a more recent building type constructed between 1991 and 2005, the corresponding values reached up to 36.47% and 75.7%.

Keywords: building energy needs; climate data; geographic information system; overheating; TRNSYS simulation; urban heat island

1. Introduction

It is well known that anthropogenic greenhouse gas (GHG) emissions into the atmosphere have continued to rise since 1950, resulting in a global average temperature increase of more than 1 °C by 2019 [1].

The combined effects of demographic growth and the continued expansion of urban areas have been identified as key factors in accelerating climate change.

Urbanization is continuously increasing; in fact, it is expected that by 2050, more than two-thirds of the world's population will live in urban areas [2]. Currently, cities consume over 65% of global energy and generate over 70% of global CO_2 emissions [3]. The building sector is responsible for about 30% of the global energy consumption and about 27% of the total energy sector's CO_2 emissions [4]. In order to reduce the environmental impact of the building sector, it is necessary to promote the construction of new energy-efficient buildings and invest in the energy requalification of the built heritage.

In urban areas, a microclimatic phenomenon often occurs: the so-called urban heat island (UHI). This leads to local overheating. It is worthy to distinguish between surface [5,6]

and atmospheric [7–9] heat islands because the temperatures are different at the surface of the earth and in the atmospheric air, and they are higher above the city. When the phenomenon is monitored with remote sensing data, it is possible to identify the surface urban heat island, since the parameter studied is not the air temperature but the temperature of the earth's surface.

Considering the atmospheric UHI, an increase of up to 4–5 °C in the temperature compared to rural areas was highlighted in the literature. The increase in temperature is related to the high density of buildings, roads, and urban infrastructures, the absence of green areas, the use of building materials with a high capacity to accumulate heat, and the sizes of buildings [10].

At the same time, a greater number of heat-producing activities are concentrated in urban centers, such as traffic emissions, industries, and the heating and cooling systems of buildings. Once the causes have been defined, it is evident that the greater the extension of the urban area, the greater the risk of intensifying the heat island effect, with a temperature difference compared to rural areas that cannot be neglected [11]. The UHI effect was found to be more noticeable in extremely urbanized areas, highlighting, in some cases, the increase in the UHI coverage from 3.35% in 2005 to 8.56% in 2015, and in other ones, a mean land surface temperature difference equal to 0.75 °C from 2002 to 2014 [12,13]. Different studies have investigated how the shift from a rural to an urban land use configuration can result in an increase in the air temperature, which is an effect that is closely associated with the UHI phenomenon [14–16]. Even if there are several findings in the literature on this issue, the relationship among the UHI effect, land coverage, and land use in Italian cities still needs to be clarified, requiring further estimations and analysis under a quantitative point of view.

Several scientific works in the literature assessed the environmental conditions in Rome. The impact of heat waves in Rome was investigated by Zinzi et al. [17], analyzing climate data related to three districts, from 2015 to 2017. The authors found a UHI index increase of up to 1.5 °C, and found a correlated cooling energy consumption increase of 87%. Analyzing three years' data from 2015 to 2017, Zinzi et al. [18] observed that the atmospheric heat island in Rome is more severe in the summer (intensity of 1 °C) than in the winter (intensity of 0.7 °C). A parametrization of Rome's morphology was conducted by Morini et al. [19], highlighting that an increase in terms of an albedo can reduce the air temperature by up to 4 °C. Rome is placed about 25 km from the Tyrrhenian coast, and some investigations analyzed the correlation between the sea breeze and the urban texture of the city as they influence the atmospheric heat island [7,20–22]. Numerous studies in the literature focus on the UHI's impacts on the climatic conditions in Rome and the positive effects of the applied mitigation strategies in terms of the air temperature value reduction in localized zones and outdoor thermal comfort conditions [5,18,23].

The assessment of the intensity of the UHI phenomenon within urban areas is closely tied to the selection of the reference meteorological station. Martin et al. [24] provided a comprehensive definition of the necessary requirements that an area must satisfy in order to be categorized as a reference rural zone. Specifically, this area should be characterized by a low percentage of hard-covered surfaces (less than 10%) and be located within or in close proximity to the urban environment. Consequently, in order to properly assess the heat island phenomenon, weather stations installed in areas that are correctly defined as "rural" are needed.

In this context, the correct UHI identification matches the climate data availability issue, which, in turn, can be related to the building energy simulation topic. By combining monitoring data together with a numerical analysis, several authors studied different UHI mitigation strategies in Rome [25–28]. The effect of the UHI phenomenon on buildings' energy performances in a densely built city can be significant [29]. It is evident how accurate simulation models are fundamental to perform these kinds of studies.

The energy efficiency of the building stocks and the requalification strategies to be applied are very critical issues that have to be considered and carefully chosen. Consequently,

the employment of dynamic simulation tools for building and urban energy modeling requires suitable environmental data. Usually, dynamic software applies climate data from their library to run a building energy model, the so-called Typical Meteorological Year (TMY). Employing these datasets can reproduce geographic positions and climatic conditions for every hour in a year, considering data covering a long time period [30–32]. The selected data must be accurate to best represent the actual climatic conditions of the area in which the simulated building is located. Therefore, to assess the effects of climate change on buildings' energy efficiency and their energy consumption, depending on the urban density of the area in which they are built, updated and precise meteorological data from weather stations located within the city are needed.

Battista et al. [33] conducted a comprehensive experimental investigation of the atmospheric UHI phenomenon within the urban environment of Rome, employing data collected from a network of 23 meteorological stations. The findings obtained from this study revealed that the temperature increase related to the heat island phenomenon within the city shows a variability in space and time. Specifically, the northeastern side of the city experiences more critical climatic conditions that are associated with the UHI effect. However, in accordance with the definition of the reference rural area proposed by Martin et al. [24], it is worthy to observe that in [33], the characteristics of the areas where the Fiumicino (FCO) and Ciampino (CIA) airport stations are situated do not meet the necessary requirements. The FCO station is located in an area that is far from Rome, which may result in a different climatic domain compared to that of the city. On the other hand, the CIA station exhibits an excessively high percentage of hard covered surfaces. Therefore, considering the climatic conditions recorded at the airports may lead to errors in estimating the energy demands of buildings within the city.

This research is a preliminary follow-up of the study described in [33]. Here, climatic data (in terms of air temperature, relative humidity, and wind speed) obtained from the weather stations located in the two Roman airports (Fiumicino and Ciampino) and those recorded in different neighborhoods of Rome were acquired during 2020 and 2022, and they were analyzed and compared. Finally, a building model was created by means of the dynamic software, TRNSYS 16 [31], to evaluate and compare the atmospheric UHI intensity in these two years and its effect on the energy performance in terms of the energy needs for heating and cooling. In this work, a step forward was made in terms of selecting the rural reference weather station, using one installed in a green neighborhood of the city, which was able to better satisfy the definition proposed in the literature.

2. Aim and Scope

As already mentioned, this work is a preliminary follow-up of the investigation described in [33], where only 2020 climate data were analyzed, which was the time of the COVID-19 lockdown. In accordance with the Institute for Environmental Protection and Research (ISPRA) [34], 2020 was one of the hottest years in Italy since 1961, with an average anomaly of +1.54 °C relative to the climatic reference value of the 1961–1990 period [34].

According to a recent analysis conducted by the Institute of Atmospheric Sciences and Climate of the Italian National Research Council (ISAC-CNR), 2020 was surpassed by 2022 in terms of recorded temperatures. The year of 2022 was the hottest year in Italy since 1800, with an average temperature of 14.95 °C, which is 1.15 °C higher than the average for the period between 1991 and 2020 [35].

Starting from this, here, the atmospheric UHI in Rome was assessed through an updated analysis based on environmental data logged within the metropolitan area during 2020 and 2022, that is, the time of the COVID-19 lockdown and a normal year. The aim of this research activity is to provide revised analyses of the climatic conditions in Rome both in space and time, with constant investigations, proposing an observation of the heat island from two points of view:

- The climatic point of view, which is based on the evaluation of the diurnal and nocturnal heat island intensities in function of the reference station. However, it

is worthy to observe that the specific choice of the reference rural weather station influences the estimation of the strength of the heat island. The so-called rural station should be placed outside of the constructed urban space. Nonetheless, the urban continuum frequently lacks clear boundaries. Most cities do not border on rural spaces, but rather on peri-urban spaces. Therefore, different choices can affect UHI intensity evaluations, leading to different results in both directions (severe or modest heat island intensities).

- The second one is the building energy point of view. It is well known that the UHI affects the climatic conditions within a city. On the other hand, buildings' energy simulations are often performed using the Typical Meteorological Year (TMY), which comprises statistically processed climatic data related to specific geographic locations, whose data come from airport monitoring. On the other hand, if calibrated energy models are required, it is necessary to rely on updated weather data acquired in the desired time windows and registered in meteorological stations near the building that is considered as the case of study. The use of weather data registered outside of the city (commonly airport sites) can lead to the effect of the UHI phenomenon on the energy performance of the building being neglected, and can consequently lead to an incorrect estimation of the energy needs for heating and cooling. This issue could be stressed when the different neighborhoods of cities are characterized by quite different environmental conditions.

3. Materials and Methods

The aim of this work is to investigate the UHI phenomenon evolution over space and time within the city of Rome (Italy), while also providing evidence of its effects on the energy performances of buildings in terms of their heating and cooling demands. Climatic data logged within and near Rome in 2020 and 2022 were analyzed in order to assess the evolution of the atmospheric UHI phenomenon over space and time within the city. In particular, the weather data analyzed in this research were measured by meteorological stations located within the city and by two meteorological stations installed in the airports of Ciampino and Fiumicino, respectively. The UHI phenomenon also has implications in terms of the energy performances of buildings. Often, airport data are used in energy simulations in order to investigate the energy performances of buildings. However, airports can be located outside of the urban context, providing data that may not consider the UHI phenomenon.

3.1. Methodology

As mentioned before, this research is a follow-up of the study described in [33], where the highest urban heat island intensity (UHII) values were identified in the northeastern side of the city. Starting from this, considering the availability of updated climate data, here, four Weather Stations (WSs) selected within the ones available in that area were employed. Figure 1 shows their positions and the locations of the two airports. Different colors and marker shapes were used to distinguish urban and airport weather stations. Yellow square markers were used for airports, and circle orange markers were used for urban stations. It is worthy to observe that the urban station, WS1, in Figure 1 is characterized by a circle marker with a yellow-orange tint. This graphic solution has been used to specify that the urban station is in a rather green area of the city, in a context that could be defined as rural (or semi-rural), and this urban station was also used as a reference to evaluate the UHI intensity. For the sake of clarity, the UHI intensity can be evaluated as the difference between air temperatures measured in an urban context and air temperatures measured in a rural zone. Consequently, the intensity of the UHI is expressed in the temperature difference at a given time between the hottest area of a city and the non-urban space surrounding it. The information on the geographical positions of the selected meteorological stations is listed in Table 1.

Figure 1. Locations of the weather stations.

Table 1. Districts, acronyms, and coordinates of the weather stations.

District	Acronym	Coordinates
Fiumicino	FCO	41°47′53.66″ N, 12°14′22.36″ E
Ciampino	CIA	41°48′29.49″ N, 12°35′5.82″ E
Roma—Tor Carbone	WS1	41°49′46.6″ N, 12°32′28.3″ E
Roma—Vigna Clara	WS2	41°56′39.6″ N, 12°27′39.0″ E
Roma—San Pietro	WS3	41°54′13.7″ N, 12°26′38.0″ E
Roma—Trieste	WS4	41°55′29.9″ N, 12°30′49.7″ E

The methodological approach of this work is characterized by the following main steps:

1. Weather data recording and GIS analysis: Climatic data (recorded in 2020 and 2022) in terms of air temperature, wind speed, and relative humidity were acquired for the selected points, and a GIS analysis was performed. The analysis was conducted using QGIS 3.28, an open-source GIS application that allows one to visualize, organize, analyze, and represent spatial data. A circular area centered around the meteorological station, with a diameter equal to 2.8 km, was defined, and the land use map of the Urban Atlas 2018 [36], provided by the Earth observation program of the European Union Copernicus [37], was considered. In this way, it was possible to identify the surfaces that correspond to buildings, or those that are covered by water, greenery, and roads or other hard surfaces (e.g., sidewalks and squares).

2. Weather data analysis: By examining the air temperature, wind speed, and relative humidity values, it was possible to characterize the climatic conditions in the selected areas during the considered periods. Consequently, a comparison was made between the results for the two years.

3. UHI assessment and reference station issue: FCO and CIA climatic data were preliminarily used as references to compute the UHI intensity (UHII). As mentioned before, airport data were used to evaluate the UHI impact on heating and cooling energy demands of buildings. The UHIIs were calculated by processing the monthly average maximum and minimum air temperatures during the day and night. The UHII values during the day and night were calculated as follows [33]:

$$UHII_{day} = T_{max,UA} - T_{max,RA} \qquad (1)$$

$$UHII_{night} = T_{min,UA} - T_{min,RA} \qquad (2)$$

where the maximum and minimum monthly values are represented with the max and min subscripts, respectively, while the urban areas' data and rural areas' data are represented with UA and RA. Finally, the urban station, WS1, positioned in a rather green area of the city, in a context that could be defined as rural (or semi-rural), was also used as a reference station to evaluate the UHII.

4. Building energy simulations: The meteorological data acquired from the weather stations in Rome, CIA, and FCO, were used as thermal boundary conditions for the simulations of the annual energy needs for the heating and cooling of two typical buildings using TRNSYS [31]. Simulations were carried out considering two separate Italian residential buildings with 72 m^2 floor area. The first building is characterized by a typical stratigraphy covering the construction period of 1900–1950 (named in the following as B1), with bricks plastered on both sides [38] (thermal conductivities of bricks and plaster equal to 0.770 W/mK and 0.700 W/mK, respectively). The second one is characterized by a typical stratigraphy for the construction period of 1991–2005 (named in the following as B2), with walls made of concrete (thermal conductivity of 1.900 W/mK) with a thickness of 0.30 m, thermally insulated with 0.06 m extruded polystyrene panels (thermal conductivity of 0.045 W/mK) and plastered on both sides (thermal conductivity of plaster equal to 0.700 W/mK). Table 2 lists the main characteristics of the two buildings modeled with TRNSYS, according to previous works [11,33].

Table 2. Main characteristics of the two building models.

	Building 1 (B1)	**Building 2 (B2)**
Construction period	1900–1950	1991–2005
Building shape	Cubic-shaped structure with horizontal roof	Cubic-shaped structure with horizontal roof
Wall thermal resistance	0.810 m^{2}K/W	1.496 m^{2}K/W
Solar absorption coefficient of external walls	0.6	0.6
Windows' thermal transmittance	5.60 W/m^{2}K	5.60 W/m^{2}K
Infiltration rate	0.5 1/h	0.5 1/h
Internal sensible and latent heat loads	65 W and 55 W	65 W and 55 W
Internal heat gains	140 W	140 W
Indoor set point temperatures	20 °C (winter) and 26 °C (summer)	20 °C (winter) and 26 °C (summer)

The selection of these two building types is related to the regulatory framework connected with the energy efficiency that began in Italy in 1976. Italy introduced the first energy efficiency regulation with Law n.373 of 1976 [39], specifying minimum requirements for the thermal insulation of buildings and the design of thermal systems. Later, with Law n.10 of 1991 [40], additional regulations were introduced to the planning methods and the management of the building-plant system. In this regulatory context, about two-thirds of the existing Italian buildings were built before 1976. Accordingly, the selected building types set the lower and upper boundaries for most of the building stock.

Monthly average climatic data were used in TRNSYS through the Type 54 weather generator, which was used within the building model to obtain the weather data for simulations [41]. It is worthy to specify that the Type 54 generator allows for hourly climatic data to be generated from monthly average observations.

Figure 2 schematically represents the methodological approach through a flowchart that connects the several steps. Following the proposed scheme, it is possible to consider other cities or deepen the study of the UHI phenomenon in Rome by considering more stations or different time periods.
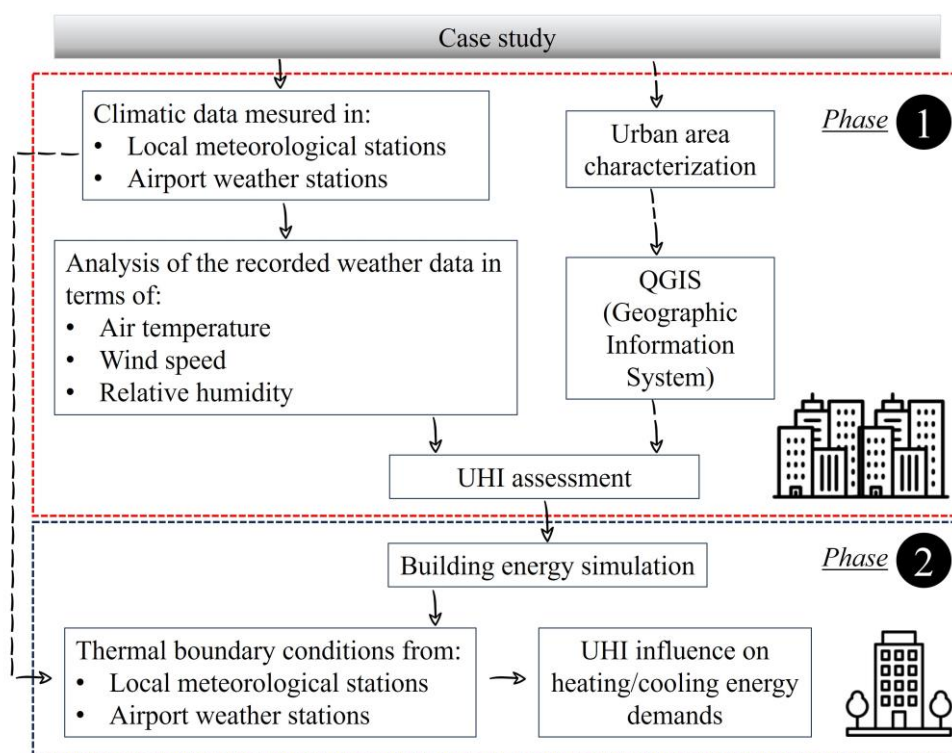
Figure 2. Flowchart of the methodological approach.

4. Results and Discussion

4.1. GIS Analysis and Climatic Conditions in the Urban Areas

It is known that the UHI phenomenon is closely related to the level of urbanization and the specific attributes of an urban environment. The principal factor contributing to the UHI is the conversion of natural open lands into urbanized areas that are characterized by the presence of buildings, roads, and surfaces constructed with massive materials. In this context, the need to understand the characteristics of the urban environment becomes evident. To obtain a comprehensive characterization of the areas where the meteorological stations are installed, in accordance with a study conducted by Battista et al. [33], an area with a 2.8 km diameter centered around each weather station was analyzed to compute the percentages of buildings, streets, green areas, and water surfaces. The characterization of the areas was performed using QGIS (a free open-source geographic information system). The land use map, Urban Atlas 2018, was used for this purpose. Figure 3 shows the in-flight views of the areas surrounding the four weather stations sited within the city, as well as the two airport sites. Figure 4 shows the percentage distribution of built-up areas, roads, and green spaces for each area. As previously stated, for this study, the climatic data recorded at the WS2, WS3, and WS4 stations were selected due to their locations in areas of the city where the impacts of the UHI phenomenon are potentially more pronounced. As expected, these areas are characterized by hard covered surfaces (built-up areas and road areas), resulting in significantly low ground permeability. In particular, the neighborhoods related to the WS2, WS3, and WS4 stations have notable shortages of green areas, with percentages ranging from 15% to 25%. Conversely, these areas are characterized by a significant presence of hard covered surfaces, with values ranging from 55% to 58% in terms of built-up areas, and from 16% to 27% in terms of street areas. The WS1 station is located within the city in a green area known as the Natural Regional Park of Appia Antica. It is characterized by extensive green surfaces, which constitute 60% of the total coverage.

Figure 3. In-flight views of all urban weather stations and the two airports.
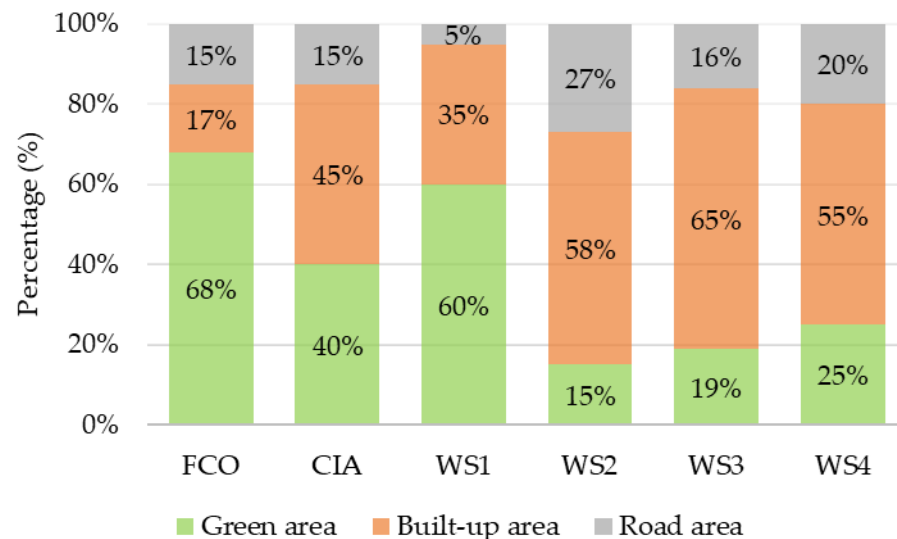

Figure 4. Green, built-up, and road areas' percentage distributions.

According to Martin et al. [24], the reference station should be placed in a rural area in close proximity to the city and characterized by natural vegetation cover. The Fiumicino and Ciampino weather stations are in a peri-urban areas outside of the city. The area of the Fiumicino station is characterized by a significantly higher percentage of green areas, accounting for 68%, compared to the Ciampino station, which has a percentage of green area equal to 40%. Conversely, the percentage of hard covered areas in Ciampino, measuring 60%, is higher than that calculated for the Fiumicino station, which stands at 32%. The area surrounding the Fiumicino weather station exhibits characteristics that are apparently consistent with those of a rural reference zone, but it is characterized by excessively large hard surfaces (not less than 10%), and it is not located within or in close proximity to the urban environment. These conditions are against what is suggested by Martin et al. [17]. Moreover, it is worth noting that the climatic domain in the Fiumicino area may differ from that in the city of Rome, given the considerable distance between the two locations, which is about 25 km [24]. In contrast, despite the proximity of Ciampino Airport to Rome, which is approximately 11 km from the city center, the surfaces of the Ciampino area are characterized by low ground permeability. This condition is correlated

to the significant presence of streets and built-up areas. Consequently, the characteristics of the area in which the Ciampino station is located do not satisfy the required criteria to designate it as a reference rural zone. Consequently, employing the climatic data recorded at the Ciampino station as a reference may lead to an inaccurate assessment of the UHI within the city.

In this context, selecting the WS1 station as a reference could be considered a viable solution due to the characteristics of the area (percentage of green areas) and its geographical position (inside the city).

The meteorological data, in terms of the air temperature, wind speed, and relative humidity, recorded in the four weather stations in Rome and in the airport stations of FCO and CIA, were analyzed, and they are shown in Figure 5. In particular, the red area represents the range of data between the maximum and minimum values measured in the weather stations within Rome in 2020, while the blue area represents the values related to 2022 recorded in the same stations. On the other hand, the red lines and the blue lines illustrate the data recorded by the airport's weather stations in 2020 and 2022. By analyzing the results, it is possible to observe that the air temperatures in Rome are higher than those measured in the two airports (Figure 5a).
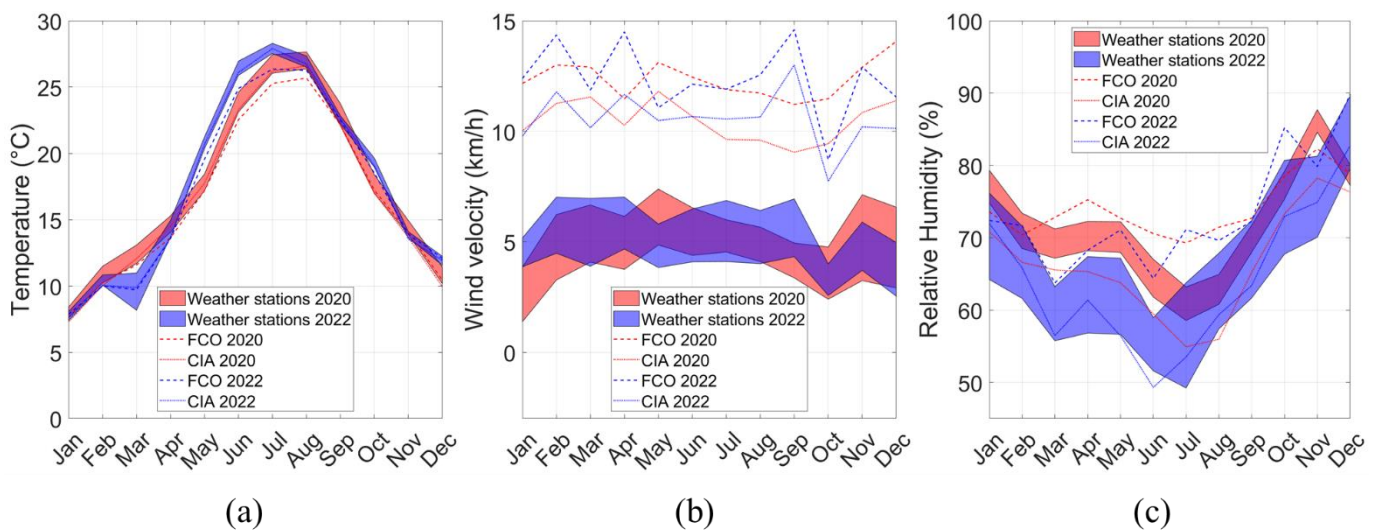

Figure 5. Monthly average values of (**a**) air temperature, (**b**) wind speed, and (**c**) relative humidity monitored during 2020 and 2022.

By analyzing the 2020 data, the maximum air temperatures measured in the CIA and FCO airport stations were equal to 26.60 °C and 26.68 °C, respectively. On the contrary, the minimum air temperatures were equal to 7.29 °C and 7.68 °C, respectively. Considering the air temperatures logged within the metropolitan area, all of the weather stations acquired higher values than the airport sites, with the maximum value registered by WS3 in August (27.65 °C).

In 2022, the maximum air temperatures measured in CIA and FCO were equal to 27.90 °C and 26.35 °C, respectively. On the other hand, minimum air temperatures equal to 7.58 °C and 7.87 °C were measured, respectively. Taking into account the air temperatures registered within the city, the maximum value of 27.65 °C was registered by WS3 in July.

The wind speed data recorded in 2020 and 2022 at the airport stations are characterized by consistently higher values than the city stations (see Figure 5b). In 2020, the wind velocity values varied from 1.38 km/h to 7.38 km/h in Rome, from 9.05 km/h to 11.81 km/h in CIA, and from 11.22 km/h to 14.06 km/h in FCO. Instead, in 2022, values ranging from 2.54 km/h to 7.02 km/h were observed in Rome, from 7.74 km/h to 13.00 km/h in CIA, and from 8.71 km/h to 14.60 km/h in FCO. These differences are due to the specific urban landscapes of the airport areas, which are characterized by lower building densities, with buildings that are not as tall as those in the city. Buildings impact the wind patterns and

decrease the airflow within the city, resulting in lower recorded wind velocities compared to the airports.

The results obtained in terms of relative humidity (RH) are shown in Figure 5c. In Rome, the RH values varied between 58.55% and 87.70% in 2020, and between 42.22% and 89.58% in 2022. The RH ranged from 54.92% to 78.23% in CIA and from 69.27% to 82.30% in FCO in 2020. In 2022, the relative humidity ranged from 49.30% to 82.71% in CIA and from 63.74% to 89.84% in FCO. These ranges are justified by the different distances from the Tyrrhenian coast and the differences in terms of green areas (see Figure 4).

The results highlight that the air temperature inside cities is higher than that measured in rural areas, such as airports. This can be attributed to the high building density, the lack of green areas, and the extensive use of massive materials.

4.2. Assessment of UHII Effects

As mentioned in Section 3.1, the UHI intensity values were initially computed by comparing the air temperature data recorded within the city (WS1, WS2, WS3, and WS4) with those measured in the airports. This analysis included both day and night data from 2020 and 2022. The daytime and night-time UHIIs were obtained by applying Equations (1) and (2). The UHII baseline was set at a value of zero (0) and represents the case for which the maximum or minimum air temperature measured within the city is the same as that of CIA or FCO.

Figure 6 shows the results obtained in 2020 by comparing the climatic data of Rome with those of the CIA and FCO stations, respectively. The yellow and the green areas represent the diurnal and nocturnal UHIIs considering all of the urban weather stations, respectively, and the two dashed lines refer to the annual average intensities. In Figure 6a, it is possible to observe that the annual average diurnal UHII value is above the baseline (2.09 °C). On the contrary, the average nocturnal UHII is below zero (−0.24 °C), highlighting that the metropolitan area is colder than the CIA airport district, on average.

The UHI is a predominantly nocturnal phenomenon, and this finding contrasts with what has been highlighted in the literature. Indeed, other studies reported night-time UHIIs in Rome ranging from 0.23 °C to 1.30 °C [11,33]. This makes it clear that the phenomenon is dynamic over time and can be correlated to specific climatic conditions. Figure 6b shows the urban heat island intensities computed while considering FCO as a reference. In this case, the annual average UHIIs calculated during the day and night show positive values: 2.34 °C for daytime and 0.30 °C for night-time.

On the other hand, the results related to 2022 are reported in Figure 7, where always positive UHIIs can be observed. Considering CIA as a reference, average annual diurnal and nocturnal UHIIs of 0.75 °C and 0.44 °C were found, respectively. On the other hand, considering FCO as a reference, 1.26 °C and 1.00 °C were obtained as annual diurnal and nocturnal heat island intensities. These results are in accordance with the findings in the literature mentioned before [11,33].

As mentioned in the Methods section, the urban station, WS1, was also used as a reference to evaluate the UHIIs, and the results are shown in Figure 8. Also, in this case, positive UHII values were obtained. In 2020, 0.58 °C and 0.99 °C were found as annual average diurnal and nocturnal UHIIs. In 2022, these values became equal to 0.24 °C and 0.56 °C. It is worthy to observe that the choice of this reference station, within a green urban context, allows for the characterization of the heat island in Rome with modest diurnal and nocturnal intensity values (lower than 1 °C) on average. During the 2020 summer months (June, July, and August), the highest UHII values reached about 1.40 °C and 2.00 °C during the day and night, respectively. In 2022, these values became equal to about 0.60 °C and 2.00 °C.

In Figure 9, a comprehensive summary of all of the obtained results in terms of the UHII values is presented, specifically referring to the years 2020 and 2022. Analyzing the results, it is possible to observe that the particular selection of the reference meteorological station allows for different intensities of the UHI during the day or during the night to be

found. Specifically, when selecting the Fiumicino meteorological station as a reference, the UHI phenomenon appears to be predominantly diurnal. Conversely, when considering WS1 as a reference, the UHI phenomenon predominantly occurs at night, which is in accordance with other works in the literature [42,43].

Figure 6. (**a**) Day and night UHIIs in 2020 considering CIA as reference. (**b**) Day and night UHIIs in 2020 considering FCO as reference.

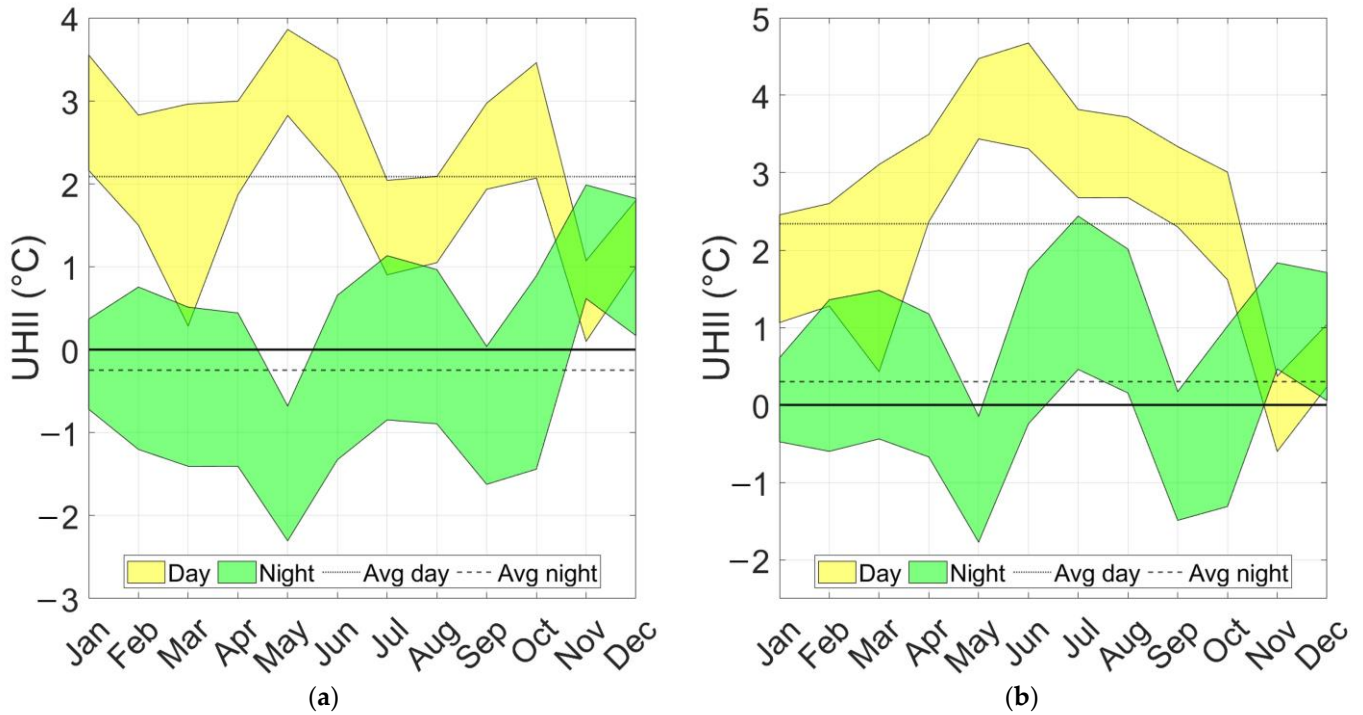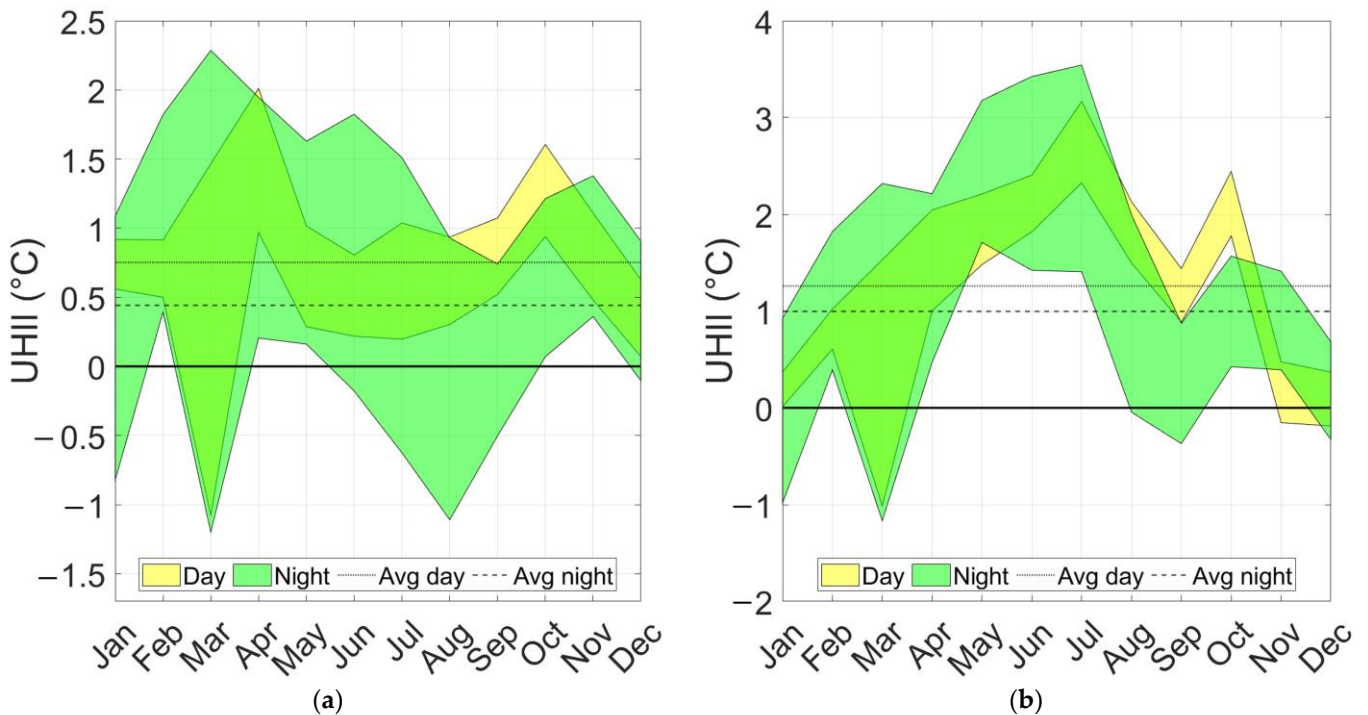**Figure 7.** (**a**) Day and night UHIIs in 2022 considering CIA as reference. (**b**) Day and night UHIIs in 2022 considering FCO as reference.
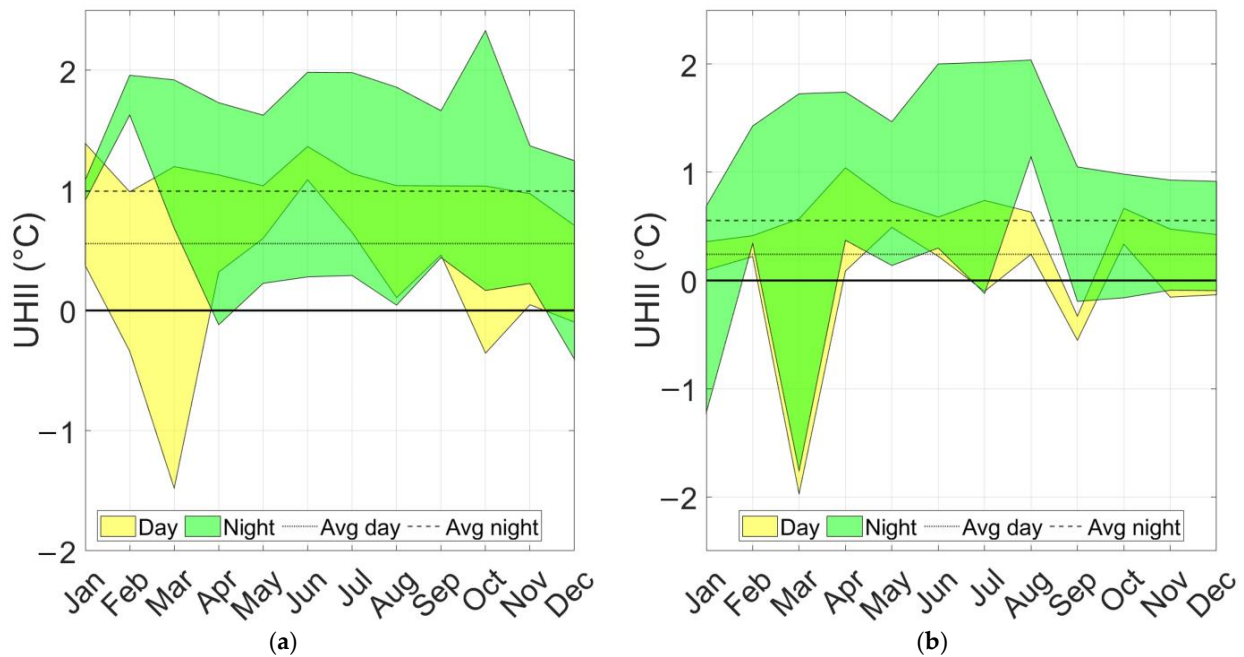
Figure 8. (**a**) Day and night UHIIs in 2020 (**a**) and 2022 (**b**) considering WS1 as reference.

Time	FCO day 2020				FCO night 2020				CIA day 2020				CIA night 2020				WS1 day 2020			WS1 night 2020		
	WS1	WS2	WS3	WS4	WS1	WS2	WS3	WS4	WS1	WS2	WS3	WS4	WS1	WS2	WS3	WS4	WS2	WS3	WS4	WS2	WS3	WS4
Jan	1.06	1.44	2.45	1.44	-0.48	0.44	0.61	0.56	2.16	2.54	3.55	2.53	-0.72	0.20	0.37	0.32	0.38	1.39	0.37	0.92	1.09	1.03
Feb	1.61	1.28	2.60	1.51	-0.60	1.03	1.22	1.36	1.84	1.50	2.83	1.73	-1.20	0.42	0.61	0.75	-0.34	0.99	-0.11	1.63	1.82	1.96
Mar	1.91	1.91	3.11	0.43	-0.44	0.25	1.48	1.10	1.76	1.76	2.96	0.28	-1.41	-0.72	0.51	0.13	0.00	1.20	-1.48	0.68	1.92	1.54
Apr	2.37	2.96	3.50	2.69	-0.55	-0.67	1.18	-0.18	1.87	2.46	3.00	2.19	-1.29	-1.41	0.44	-0.91	0.59	1.13	0.32	-0.12	1.73	0.38
May	3.44	4.04	4.47	4.15	-1.77	-1.55	-0.15	-1.16	2.82	3.42	3.86	3.53	-2.30	-2.08	-0.68	-1.69	0.60	1.04	0.71	0.23	1.63	0.62
Jun	3.31	4.40	4.67	4.45	-0.24	0.04	1.74	0.45	2.13	3.21	3.49	3.26	-1.33	-1.05	0.66	-0.63	1.09	1.37	1.14	0.28	1.98	0.70
Jul	2.68	3.33	3.82	3.55	0.46	0.75	2.44	1.03	0.90	1.55	2.04	1.78	-0.85	-0.56	1.13	-0.28	0.65	1.14	0.88	0.29	1.98	0.57
Aug	2.68	2.79	3.72	3.31	0.15	0.20	2.01	0.61	1.05	1.16	2.09	1.68	-0.89	-0.85	0.96	-0.44	0.11	1.04	0.63	0.04	1.86	0.46
Sep	2.30	2.76	3.34	3.03	-1.49	0.17	-0.01	-1.05	1.93	2.40	2.97	2.66	-1.62	0.04	-0.14	-1.18	0.46	1.04	0.73	1.66	1.49	0.44
Oct	1.97	1.62	3.01	2.36	-1.31	1.02	0.29	-1.15	2.42	2.07	3.46	2.81	-1.44	0.89	0.16	-1.27	-0.35	1.04	0.39	2.33	1.60	0.17
Nov	-0.60	-0.55	0.37	-0.49	0.46	0.69	1.84	0.79	0.10	0.15	1.07	0.21	0.61	0.84	1.99	0.94	0.05	0.97	0.11	0.23	1.37	0.33
Dec	0.33	0.24	1.04	0.44	0.46	0.06	1.71	0.55	1.09	0.99	1.80	1.20	0.58	0.17	1.82	0.66	-0.10	0.71	0.11	-0.41	1.25	0.09

(a)

Time	FCO day 2022				FCO night 2022				CIA day 2022				CIA night 2022				WS1 day 2022			WS1 night 2022		
	WS1	WS2	WS3	WS4	WS1	WS2	WS3	WS4	WS1	WS2	WS3	WS4	WS1	WS2	WS3	WS4	WS2	WS3	WS4	WS2	WS3	WS4
Jan	0.01	0.30	0.11	0.37	0.24	0.36	0.93	-0.98	0.56	0.85	0.66	0.92	0.40	0.53	1.09	-0.82	0.29	0.10	0.36	0.13	0.69	-1.22
Feb	0.61	1.02	0.92	0.83	0.39	0.74	1.82	0.76	0.50	0.91	0.81	0.72	0.39	0.74	1.82	0.76	0.41	0.31	0.22	0.34	1.43	0.36
Mar	0.96	1.53	1.13	-1.01	0.59	0.99	2.32	-1.17	0.90	1.47	1.07	-1.08	0.56	0.96	2.29	-1.20	0.57	0.17	-1.97	0.40	1.73	-1.76
Apr	1.00	1.53	1.09	2.04	0.47	0.84	2.21	1.35	0.97	1.49	1.06	2.01	0.20	0.58	1.95	1.09	0.52	0.09	1.04	0.37	1.74	0.88
May	1.48	2.21	1.97	2.08	1.71	2.01	3.18	1.85	0.29	1.02	0.78	0.89	0.16	0.46	1.63	0.30	0.73	0.49	0.60	0.30	1.47	0.14
Jun	1.82	2.10	2.41	2.04	1.42	1.72	3.42	1.75	0.22	0.50	0.81	0.44	-0.18	0.12	1.82	0.15	0.29	0.59	0.22	0.30	2.00	0.33
Jul	2.43	2.98	2.33	3.17	1.53	1.82	3.54	1.41	0.30	0.85	0.20	1.04	-0.51	-0.21	1.51	-0.63	0.55	-0.10	0.74	0.29	2.02	-0.12
Aug	1.50	2.13	1.98	1.74	-0.05	1.10	1.99	1.52	0.30	0.94	0.79	0.55	-1.11	0.03	0.93	0.45	0.63	0.48	0.24	1.14	2.04	1.56
Sep	1.44	1.11	1.04	0.89	-0.18	-0.37	0.87	0.14	1.07	0.74	0.67	0.52	-0.31	-0.50	0.74	0.01	-0.33	-0.40	-0.55	-0.19	1.05	0.32
Oct	1.78	2.37	2.44	2.11	0.58	0.47	1.57	0.42	0.94	1.53	1.61	1.28	0.23	0.12	1.21	0.07	0.59	0.67	0.34	-0.11	0.98	-0.16
Nov	0.00	-0.01	0.48	-0.15	0.48	0.39	1.41	0.47	0.63	0.62	1.11	0.48	0.45	0.36	1.38	0.44	-0.01	0.48	-0.15	-0.09	0.93	-0.01
Dec	-0.05	0.12	0.37	-0.19	-0.24	-0.31	0.68	-0.33	0.20	0.38	0.63	0.07	-0.01	-0.08	0.91	-0.10	0.18	0.42	-0.13	-0.07	0.92	-0.09

(b)

Figure 9. (**a**) Day and night UHIIs in 2020 considering FCO, CIA, and WS1 as references. (**b**) Day and night UHIIs in 2022 considering FCO, CIA, and WS1 as references (the orange and blue boxes identify the maximum and minimum values).

4.3. Building Energy Simulations

Simulations were performed using TRNSYS by reproducing two representative residential buildings in Italy (named in the following as B1 and B2). The aim was to evaluate the effects of the UHI phenomenon on the annual energy demands for heating and cooling. Figures 10 and 11 provide an overview of the simulation outcomes, specifically presenting the total heating and cooling energy needs per unit floor area, which were computed using different meteorological datasets based on the logged data during 2020 and 2022. The results highlight that the energy demands for heating are higher in areas outside of Rome (CIA and FCO) and in greener urban area, such as WS1. These findings highlight that during the winter, the UHI has a positive influence by decreasing the energy demands for heating. Conversely, the analysis confirmed that the energy requirements for cooling are higher in densely built areas. As expected, the simulated energy demands for the typical B1 building differed from those obtained for building B2 because of different thermal insulation levels.
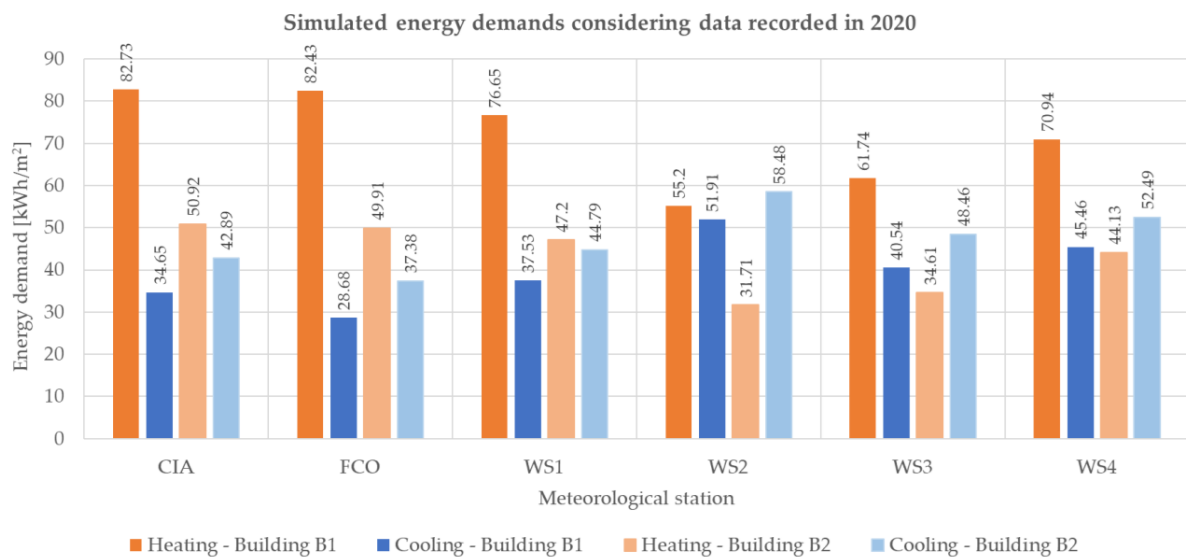
Figure 10. Heating and cooling energy demand intensities using different weather data recorded in 2020 for B1 and B2.
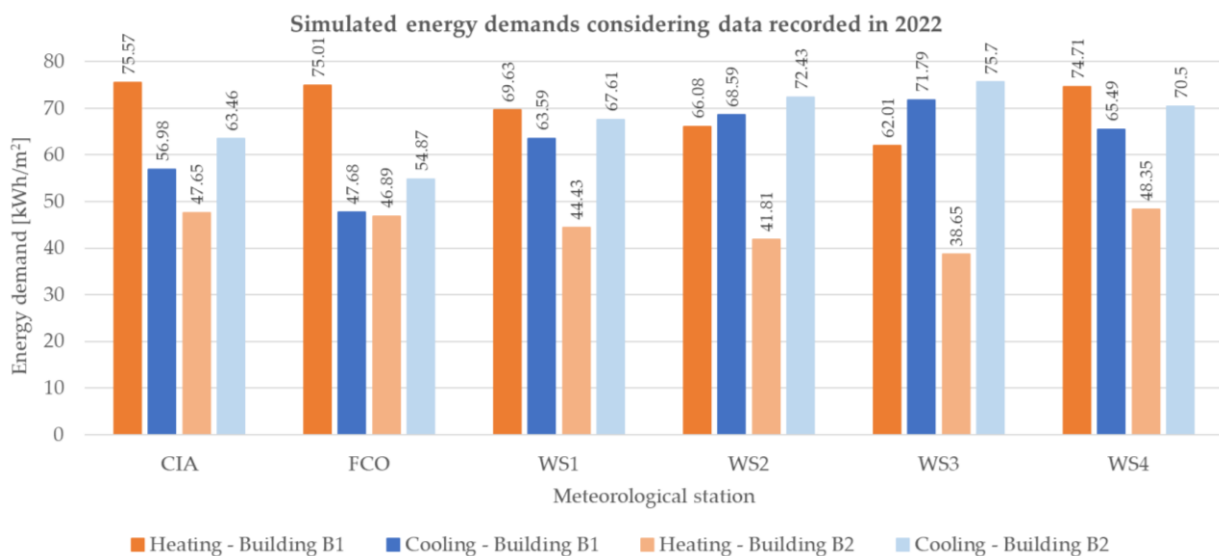
Figure 11. Heating and cooling energy demand intensities using different weather data recorded in 2022 for B1 and B2.

When using the 2020 climatic data, analyzing the results obtained for B1, and considering FCO as a reference, it is possible to notice heating energy demands varying from −33.0% to 0.4%. When CIA is considered as a reference, quite similar percentage differences can be obtained, from −33.3% to −0.4%. On the other hand, when analyzing the cooling energy needs for 2020 while considering FCO as a reference, a variation in terms of the heating energy demands ranging from 20.8% and 81.0% is found. When CIA is considered as a reference, the percentage differences range from −17.2% to 49.8%. Finally, considering WS1 as reference and analyzing the heating energy needs simulated using only the weather data related to WS2, WS3, and WS4, the percentage differences range between −28.0% and −7.4%. These values become equal to 21.1% and 38.3% when the energy needs for cooling are considered. On the other hand, when considering B2 and FCO as references, heating energy demand variations from −36.5% to 2.0% were computed. When taking CIA as a reference, similar differences can be observed, from −37.7% to −2.0%. When analyzing the cooling energy demands, when FCO is the reference climatic dataset, a variation for heating ranging from 14.7% to 56.4% is found. Considering CIA as a reference, the differences vary from −12.8% to 36.3%. Finally, considering WS1 as a reference and analyzing the heating energy needs, the percentage differences range between −32.8% and −6.5%. These values become equal to 8.2% and 30.6% when the energy needs for cooling are considered.

By applying the 2022 climatic data, when B1 is simulated, taking FCO as a reference, it is possible to notice heating energy demands varying from −17.3% to 0.7%. When CIA is considered as a reference, quite similar percentage differences can be obtained, from −17.9% to −0.7%. Finally, considering WS1 as a reference and analyzing the heating energy needs that were simulated using only the urban weather data, the percentage differences range between −5.1% and 7.3%. These values become equal to 3.0% and 12.9% when the energy needs for cooling are considered. On the other hand, when analyzing the cooling energy needs, considering FCO as a reference, a variation in terms of heating energy demands ranging from 19.5% and 50.6% is found. When CIA is considered as a reference, the percentage differences range from −16.3% to 26.0%. Considering B2 and FCO as references, heating energy demand variations from −17.6% to 3.1% are calculated. Taking CIA as a reference, quite similar differences can be observed, from −18.9% to 1.5%. When analyzing the cooling energy demands, when FCO is the reference climatic dataset, a variation in terms of heating energy demands ranging from 15.7% to 38.0% is found. Considering CIA as a reference, the differences vary from −13.5% to 19.3%. Finally, considering WS1 as a reference and analyzing the heating energy needs, the percentage differences range between −13.0% and 8.8%. These values become equal to 4.3% and 12.0% when the energy needs for cooling are considered.

The results allow us to highlight the impact of the building envelope's construction characteristics on the energy performance. The higher thermal resistance of the walls in the more modern building type (B2) led to a significant reduction in the heating energy demand compared to the older building typology (B1). However, the cooling energy demand values for building B2 were found to be higher than those for building B1.

Aiming to provide a comparison with the existing literature, considering the FCO station as a reference, an average decrease in terms of the annual heating energy demand of about −16% can be noticed for 2020, and an average decrease of about −7% can be seen for 2022. On the contrary, an average increase of about 47% is found for cooling during 2020 and about a 37% increase is found during 2022. These data can be compared with the previous works related to the climatic conditions in Rome and their influences on buildings' energy performances. A heating energy demand reduction ranging from about −18% to −16% was highlighted using the climate data related to the time span of 2014–2020 [11,33] due to the UHI phenomenon in Rome. On the contrary, the data from the literature reveal an increase in the cooling energy demands from about 58% to about 67%. Starting from this, the obtained results confirmed the need to carefully address the local climatic conditions for building simulation purposes.

The findings demonstrate how particular thermal boundary conditions significantly impact the energy requirements for heating and cooling. Therefore, the careful selection of suitable reference data during simulations assumes a critical role in achieving accurate estimations of building energy requirements. This is fundamental when calibrated models are needed for buildings' energy retrofit through specific interventions designed in function of the actual buildings' thermal behaviors. Energy simulations are often performed by applying TMYs, whose data come from airport monitoring. When calibrated models are needed, it is necessary to use updated weather data logged within the desired time windows and through meteorological stations installed near the building considered as the case of study. The use of climate data acquired outside of cities (generally airport sites), can lead to the effect of the UHI phenomenon on the simulated energy performance being neglected. These aspects become crucial, especially in ancient countries like Italy, where a large part of the built heritage requires redevelopment interventions.

5. Limits of This Work

Despite the significant results, some possible weaknesses of this work that, at the same time, represent possible future developments need to be highlighted:

- Other typical wall stratigraphies can be used within building energy simulations in order to provide a wider range of constructive techniques of the building stock.
- Several construction archetypes of the Italian building heritage can be investigated in order to provide a more comprehensive view.
- It is worthy to observe that the building heating and cooling energy needs also depend on the household size, the user's behavior, and their lifestyle. Consequently, these issues represent food for thought for the follow-up of this research.

6. Conclusions

The UHI phenomenon in Rome was examined here while also considering its effects on building energy needs. The investigation was carried out by analyzing meteorological data collected during the years of 2020 and 2022. The Fiumicino and Ciampino airports were preliminary selected as reference stations to calculate the heat island intensities because energy simulation software generally exploits airport climate data, leading to a potential neglect of the effect of the UHI on the building's energy performance and consequently leading to an incorrect estimate of the energy consumption.

In 2020, when considering the FCO station as a reference, the annual average UHIIs calculated for the day and night showed positive values, which were 2.34 °C for daytime and 0.30 °C for night-time. Instead, considering CIA as a reference, an annual average diurnal UHII of 2.09 °C was obtained, while the nocturnal UHII was equal to −0.24 °C, highlighting that the metropolitan area is colder than the CIA airport district, on average. The negative heat island intensity value raises some questions about the selection of the Ciampino airport site as a possible reference station. The characteristics of the area in which the CIA station is installed do not align with the definition of rural area provided in the literature. Finally, the urban station, WS1, which is positioned in a rather green area of the city, in a context that could be defined as rural (or semi-rural), was also used as a reference to evaluate the UHII. In this case, the diurnal and nocturnal UHIIs were equal to 0.58 °C and 0.99 °C, respectively.

In 2022, when selecting CIA as a reference, average annual diurnal and nocturnal UHIIs of 0.75 °C and 0.44 °C were found, respectively. Instead, considering FCO as a reference, 1.26 °C and 1.00 °C were obtained as the annual diurnal and nocturnal intensities. By choosing WS1 as a reference, the UHIIs became equal to 0.24 °C (diurnal) and 0.56 °C (nocturnal).

The assessment of the UHI intensity is strictly related to the selection of the reference weather station. The results allow us to conclude that Rome is affected by the heat island phenomenon, but more in-depth studies must be conducted to better identify the reference weather station.

By analyzing the effects of the UHI intensity on the energy needs of buildings, it is possible to state that the atmospheric heat island allows for reductions of up to approximately −33% in terms of the energy needs for heating, and it allows for an increase of up to approximately 80% for cooling based on the environmental conditions of the specific year.

The obtained results confirmed that it is not recommended to use meteorological data derived from airports, as this can lead to inaccurate estimations of the energy demands of buildings in urban environments. Failure to consider the UHI phenomenon can lead to inaccuracies. To ensure reliable results within a densely built environment, it is crucial to use climatic data recorded near the case of study. This becomes particularly valuable when evaluating energy savings resulting from renovations of existing buildings, as dynamic models can be appropriately calibrated. By utilizing calibrated models, more informed and rational assessments of energy savings can be conducted, leading to effective decision making in improving a building's energy efficiency. The use of data that were recorded in urban meteorological stations is usually limited to weather forecasts. It would therefore be advisable to enhance the network of meteorological stations within cities to collect reliable and representative climatic data for individual urban areas in an open database. Such data can be used in building energy simulations, enabling results that consider the presence of the UHI phenomenon, as well as quantifying and monitoring the effects of the UHI within urban areas.

Future developments will regard the following: (i) the simulation of other typical wall stratigraphies to provide a wider range of constructive techniques of the building stock; (ii) the influence of household size, the user's behavior, and their lifestyle; and (iii) the comparison between the UHII values obtained through climate data and specific models, such as the Oke model.

Author Contributions: Conceptualization, E.D.C., L.E., G.B. and C.G.; Methodology, E.D.C., L.E., G.B. and C.G.; Software, E.D.C. and L.E.; Formal analysis, E.D.C. and G.B.; Resources, R.D.L.V. and F.A.; Data curation, R.D.L.V. and F.A.; Writing—original draft, E.D.C. and L.E.; Writing—review & editing, L.E., C.G., R.D.L.V. and F.A.; Supervision, R.D.L.V. and F.A. All authors have read and agreed to the published version of the manuscript.

Data Availability Statement: Data are contained within the article.

Conflicts of Interest: The authors declare no conflict of interest.

Nomenclature

BEP	Building Energy Performance
CIA	Ciampino Airport
FCO	Fiumicino Airport
GHG	Greenhouse Gas
GIS	Geographic Information System
RH	Relative Humidity
$T_{max,RA}$	Maximum Air Temperature in Rural Area
$T_{max,UA}$	Maximum Air Temperature in Urban Area
$T_{min,RA}$	Minimum Air Temperature in Rural Area
$T_{min,UA}$	Minimum Air Temperature in Urban Area
TMY	Typical Meteorological Year
UHI	Urban Heat Island
$UHII_{day}$	Diurnal Urban Heat Island Intensity
$UHII_{night}$	Nocturnal Urban Heat Island Intensity
WS	Weather Station

References

1. Wang, L.; Wang, L.; Li, Y.; Wang, J. A Century-Long Analysis of Global Warming and Earth Temperature Using a Random Walk with Drift Approach. *Decis. Anal. J.* **2023**, *7*, 100237. [CrossRef]
2. Hannah Ritchie and Max Roser. Available online: https://ourworldindata.org/urbanization (accessed on 2 November 2023).
3. Zhou, X.; Huang, Z.; Scheuer, B.; Wang, H.; Zhou, G.; Liu, Y. High-Resolution Estimation of Building Energy Consumption at the City Level. *Energy* **2023**, *275*, 127476. [CrossRef]
4. IEA Buildings. Paris, 2022. Available online: https://www.Iea.Org/Reports/Buildings (accessed on 2 November 2023).
5. Cecilia, A.; Casasanta, G.; Petenko, I.; Conidi, A.; Argentini, S. Measuring the Urban Heat Island of Rome through a Dense Weather Station Network and Remote Sensing Imperviousness Data. *Urban Clim.* **2023**, *47*, 101355. [CrossRef]
6. Wang, J.; Huang, B.; Fu, D.; Atkinson, P. Spatiotemporal Variation in Surface Urban Heat Island Intensity and Associated Determinants across Major Chinese Cities. *Remote Sens.* **2015**, *7*, 3670–3689. [CrossRef]
7. Fabrizi, R.; Bonafoni, S.; Biondi, R. Satellite and Ground-Based Sensors for the Urban Heat Island Analysis in the City of Rome. *Remote Sens.* **2010**, *2*, 1400–1415. [CrossRef]
8. Foissard, X.; Dubreuil, V.; Quénol, H. Defining Scales of the Land Use Effect to Map the Urban Heat Island in a Mid-Size European City: Rennes (France). *Urban Clim.* **2019**, *29*, 100490. [CrossRef]
9. Chowienczyk, K.; McCarthy, M.; Hollis, D.; Dyson, E.; Lee, M.; Coley, D. Estimating and Mapping Urban Heat Islands of the UK by Interpolation from the UK Met Office Observing Network. *Build. Serv. Eng. Res. Technol.* **2020**, *41*, 521–543. [CrossRef]
10. Memon, R.A.; Leung, D.Y.C.; Liu, C.-H. An Investigation of Urban Heat Island Intensity (UHII) as an Indicator of Urban Heating. *Atmos. Res.* **2009**, *94*, 491–500. [CrossRef]
11. Guattari, C.; Evangelisti, L.; Balaras, C.A. On the Assessment of Urban Heat Island Phenomenon and Its Effects on Building Energy Performance: A Case Study of Rome (Italy). *Energy Build.* **2018**, *158*, 605–615. [CrossRef]
12. Huang, Q.; Huang, J.; Yang, X.; Fang, C.; Liang, Y. Quantifying the Seasonal Contribution of Coupling Urban Land Use Types on Urban Heat Island Using Land Contribution Index: A Case Study in Wuhan, China. *Sustain. Cities Soc.* **2019**, *44*, 666–675. [CrossRef]
13. Singh, P.; Kikon, N.; Verma, P. Impact of Land Use Change and Urbanization on Urban Heat Island in Lucknow City, Central India. A Remote Sensing Based Estimate. *Sustain. Cities Soc.* **2017**, *32*, 100–114. [CrossRef]
14. Fall, S.; Niyogi, D.; Gluhovsky, A.; Pielke, R.A.; Kalnay, E.; Rochon, G. Impacts of Land Use Land Cover on Temperature Trends over the Continental United States: Assessment Using the North American Regional Reanalysis. *Int. J. Climatol.* **2010**, *30*, 1980–1993. [CrossRef]
15. Xian, G.; Crane, M. An Analysis of Urban Thermal Characteristics and Associated Land Cover in Tampa Bay and Las Vegas Using Landsat Satellite Data. *Remote Sens. Env.* **2006**, *104*, 147–156. [CrossRef]
16. Li, W.; Bai, Y.; Chen, Q.; He, K.; Ji, X.; Han, C. Discrepant Impacts of Land Use and Land Cover on Urban Heat Islands: A Case Study of Shanghai, China. *Ecol. Indic.* **2014**, *47*, 171–178. [CrossRef]
17. Zinzi, M.; Agnoli, S.; Burattini, C.; Mattoni, B. On the Thermal Response of Buildings under the Synergic Effect of Heat Waves and Urban Heat Island. *Sol. Energy* **2020**, *211*, 1270–1282. [CrossRef]
18. Zinzi, M.; Carnielo, E.; Mattoni, B. On the Relation between Urban Climate and Energy Performance of Buildings: A Three-Years Experience in Rome, Italy. *Appl. Energy* **2018**, *221*, 148–160. [CrossRef]
19. Morini, E.; Touchaei, A.G.; Rossi, F.; Cotana, F.; Akbari, H. Evaluation of Albedo Enhancement to Mitigate Impacts of Urban Heat Island in Rome (Italy) Using WRF Meteorological Model. *Urban Clim.* **2018**, *24*, 551–566. [CrossRef]
20. Colacino, M.; Lavagnini, A. Evidence of the Urban Heat Island in Rome by Climatological Analyses. *Arch. Meteorol. Geophys. Bioclimatol. Ser. B Theor. Appl. Climatol.* **1982**, *31*, 87–97. [CrossRef]
21. Mastrantonio, G.; Viola, A.P.; Argentini, S.; Universitd, L.; Sapienza, R.; Abbate, I.G.; Ocone, R.; Casonato, M. Observations of Sea Breeze Events in Rome and the Surrounding Area by a Network of Doppler Sodars. *Bound. -Layer Meteorol.* **1994**, *71*, 67–80. [CrossRef]
22. Ciardini, V.; Caporaso, L.; Sozzi, R.; Petenko, I.; Bolignano, A.; Morelli, M.; Melas, D.; Argentini, S. Interconnections of the Urban Heat Island with the Spatial and Temporal Micrometeorological Variability in Rome. *Urban Clim.* **2019**, *29*, 100493. [CrossRef]
23. Salata, F.; Golasi, I.; de Lieto Vollaro, R.; de Lieto Vollaro, A. Outdoor Thermal Comfort in the Mediterranean Area. A Transversal Study in Rome, Italy. *Build. Environ.* **2016**, *96*, 46–61. [CrossRef]
24. Martin-Vide, J.; Sarricolea, P.; Moreno-García, M.C. On the Definition of Urban Heat Island Intensity: The "Rural" Reference. *Front. Earth Sci.* **2015**, *3*, 24. [CrossRef]
25. Salata, F.; Golasi, I.; Petitti, D.; de Lieto Vollaro, E.; Coppi, M.; de Lieto Vollaro, A. Relating Microclimate, Human Thermal Comfort and Health during Heat Waves: An Analysis of Heat Island Mitigation Strategies through a Case Study in an Urban Outdoor Environment. *Sustain. Cities Soc.* **2017**, *30*, 79–96. [CrossRef]
26. Battista, G.; Pastore, E.M. Using Cool Pavements to Mitigate Urban Temperatures in a Case Study of Rome (Italy). *Energy Procedia* **2017**, *113*, 98–103. [CrossRef]
27. Costanzo, V.; Evola, G.; Marletta, L. Energy Savings in Buildings or UHI Mitigation? Comparison between Green Roofs and Cool Roofs. *Energy Build.* **2016**, *114*, 247–255. [CrossRef]
28. Marando, F.; Salvatori, E.; Sebastiani, A.; Fusaro, L.; Manes, F. Regulating Ecosystem Services and Green Infrastructure: Assessment of Urban Heat Island Effect Mitigation in the Municipality of Rome, Italy. *Ecol. Model.* **2019**, *392*, 92–102. [CrossRef]

29. Evangelisti, L.; Guattari, C.; Grazieschi, G.; Roncone, M.; Asdrubali, F. On the Energy Performance of an Innovative Green Roof in the Mediterranean Climate. *Energy* **2020**, *13*, 5163. [CrossRef]

30. Liu, S.; Kwok, Y.T.; Ren, C. Investigating the Impact of Urban Microclimate on Building Thermal Performance: A Case Study of Dense Urban Areas in Hong Kong. *Sustain. Cities Soc.* **2023**, *94*, 104509. [CrossRef]

31. TRNSYS 16. TRNSYS Transient System Simulation Tool, (n.d.). Available online: http://www.trnsys.com/ (accessed on 2 November 2023).

32. Qiu, G.; Li, H.; Zhang, Q.; Chen, W.; Liang, X.; Li, X. Effects of Evapotranspiration on Mitigation of Urban Temperature by Vegetation and Urban Agriculture. *J. Integr. Agric.* **2013**, *12*, 1307–1315. [CrossRef]

33. Battista, G.; Evangelisti, L.; Guattari, C.; Roncone, M.; Balaras, C.A. Space-Time Estimation of the Urban Heat Island in Rome (Italy): Overall Assessment and Effects on the Energy Performance of Buildings. *Build. Environ.* **2023**, *228*, 109878. [CrossRef]

34. ISPRA; Fioravanti, G. *The Climate Indicators in Italy in 2020*; ISPRA: Roma, Italy, 2021; ISBN 9788844810627.

35. Il Post Il 2022 è Stato l'anno Più Caldo in Italia Dal 1800. Available online: https://www.ilpost.it/2023/01/09/2022-Anno-Piu-Caldo-Italia/ (accessed on 2 November 2023).

36. Copernicus European's Eyes on Earth, Urban Atlas, 2018. Available online: https://land.copernicus.eu/en/products/urban-atlas/urban-atlas-2018 (accessed on 2 November 2023).

37. European Commission, Copernicus, European's Eyes on Earth, 2021. Available online: Https://www.copernicus.eu/en (accessed on 2 November 2023).

38. Corrado, V.; Ballarini, I.; Corgnati, S.P.; Talà, N. *Typology Approach for Building Stock Energy Assessment Building Typology Brochure-Italy Fascicolo Sulla Tipologia Edilizia Italiana*; Politecnico di Torino: Torino, Italy, 2011; ISBN 978-88-8202-070-5.

39. LEGGE 30 Marzo 1976, n. 373 Norme per Il Contenimento Del Consumo Energeti-Co per Usi Termici Negli Edifici. 1976. Available online: https://www.gazzettaufficiale.it/eli/id/1976/06/07/076U0373/sg (accessed on 2 November 2023).

40. LEGGE 9 Gennaio 1991, n. 10 Norme per l'attuazione Del Piano Energetico Na-Zionale in Materia Di Uso Razionale Dell'energia, Di Risparmio Energetico e Di Sviluppo Delle Fonti Rinnovabili Di Energia. 1991. Available online: https://www.gazzettaufficiale.it/eli/id/1991/01/16/091G0015/sg (accessed on 2 November 2023).

41. Hassid, S.; Santamouris, M.; Papanikolaou, N.; Linardi, A.; Klitsikas, N.; Georgakis, C.; Assimakopoulos, D.N. The Effect of the Athens Heat Island on Air Conditioning Load. *Energy Build.* **2000**, *32*, 131–141. [CrossRef]

42. Giovannini, L.; Zardi, D.; de Franceschi, M.; Chen, F. Numerical Simulations of Boundary-layer Processes and Urban-induced Alterations in an Alpine Valley. *Int. J. Climatol.* **2014**, *34*, 1111–1131. [CrossRef]

43. Founda, D.; Katavoutas, G.; Pierros, F.; Mihalopoulos, N. The Extreme Heat Wave of Summer 2021 in Athens (Greece): Cumulative Heat and Exposure to Heat Stress. *Sustainability* **2022**, *14*, 7766. [CrossRef]